Mutagenesis, 2020, 35, 161–167
doi:10.1093/mutage/geaa006
Original Manuscript
Advance Access publication 12 February 2020

OXFORD

Original Manuscript

Dextran sulfate sodium mouse model of inflammatory bowel disease evaluated for systemic genotoxicity via blood micronucleus and *Pig-a* gene mutation assays

Christopher Kirby[1], Ayesha Baig[2], Svetlana L. Avlasevich[1], Dorothea K. Torous[1], Shuchang Tian[1], Priyanka Singh[1], Jeffrey C. Bemis[1], Lawrence J. Saubermann[2] and Stephen D. Dertinger[1,*]

[1]Litron Laboratories, 3500 Winton Place, Rochester, NY 14623 and [2] Department of Pediatrics, University of Rochester Medical Center, 601 Elmwood Ave., Rochester, NY 14642

*To whom correspondence should be addressed. SDD, Litron Laboratories, 3500 Winton Place, Rochester, NY 14623. Tel: 585-442-0930; Fax: 585-442-0934; Email: sdertinger@litronlabs.com

Received 10 December 2019; Editorial decision 19 January 2020; Accepted 24 January 2020.

Abstract

Inflammatory bowel disease (IBD) is an important risk factor for gastrointestinal cancers. Inflammation and other carcinogenesis-related effects at distal, tissue-specific sites require further study. In order to better understand if systemic genotoxicity is associated with IBD, we exposed mice to dextran sulfate sodium salt (DSS) and measured the incidence of micronucleated cells (MN) and *Pig-a* mutant phenotype cells in blood erythrocyte populations. In one study, 8-week-old male CD-1 mice were exposed to 0, 1, 2, 3 or 4% w/v DSS in drinking water. The 4-week in-life period was divided into four 1-week intervals—alternately on then off DSS treatment. Low volume blood samples were collected for MN analysis at the end of each week, and cardiac blood samples were collected at the end of the 4-week period for *Pig-a* analyses. The two highest doses of DSS were observed to induce significant increases in reticulocyte frequencies. Even so, no statistically significant treatment-related effects on the genotoxicity biomarkers were evident. While one high-dose mouse showed modestly elevated MN frequencies during the DSS treatment cycles, it also exhibited exceptionally high reticulocyte frequencies (e.g. 18.7% at the end of the second DSS cycle). In a second study, mice were treated with 0 or 4% DSS for 9–18 consecutive days. Exposure was continued until rectal bleeding or morbidity was evident, at which point the treatment was terminated and blood was collected for MN analysis. The *Pig-a* assay was conducted on samples collected 29 days after the start of treatment. The initial blood specimens showed highly elevated reticulocyte frequencies in DSS-exposed mice (mean ± SEM = 1.75 ± 0.10% vs. 13.04 ± 3.66% for 0 vs. 4% mice, respectively). Statistical analyses showed no treatment-related effect on MN or *Pig-a* mutant frequencies. Even so, the incidence of MN versus reticulocytes in the DSS-exposed mice were positively correlated (linear fit R^2 = 0.657, P = 0.0044). Collectively, these results suggest that in the case of the DSS CD-1 mouse model, systemic effects include stress erythropoiesis but not remarkable genotoxicity. To the extent MN may have been slightly elevated in a minority of individual mice, these effects appear to be secondary, likely attributable to stimulated erythropoiesis.

© The Author(s) 2020. Published by Oxford University Press on behalf of the UK Environmental Mutagen Society.
All rights reserved. For permissions, please e-mail: journals.permissions@oup.com.

Introduction

Inflammatory bowel disease (IBD), including Crohn's disease (CD) and ulcerative colitis (UC), is a chronic relapsing inflammatory condition affecting mainly the gastrointestinal tract. Although the exact mechanisms underlying the initial development of IBD are not fully understood, it is believed that an abnormal immune response is elicited against the intestinal microbiota in genetically predisposed individuals exposed to environmental risk factors (1).

One deleterious consequence of IBD is an increased risk of gastrointestinal malignancies. According to the meta-analysis of population-based cohort studies reported by Jess *et al.* (2), the risk of colorectal cancer is increased 2.4-fold in patients with UC. Risk is particularly high in males, those of young age at diagnosis with UC, and those with extensive colitis. After approximately 8–10 years after diagnosis, the risk begins to increase significantly above that of the general population. For example, a meta-analysis conducted by Eaden *et al.* (3) reported that colorectal cancer risk in UC is 2% after 10 years, 8% after 20 years and 18% after 30 years of the disease. The overall survival is driven primarily by age, comorbidities and cancer stage at diagnosis (4).

Prolonged chronic inflammation is assumed to be a causative factor in colitis-associated gastrointestinal carcinomas (5). As reviewed by Hanahan and Weinberg (6), local inflammation is considered a hallmark of cancer and likely contributes to neoplastic transformation in several ways, e.g. by enhancing angiogenesis and risk of metastasis as the result of extracellular matrix degradation, and through genetic alterations caused by reactive oxygen and nitrogen species.

While the IBD/cancer link is obvious for gastrointestinal tissues, it is less clear for distal sites. While increased risk of non-melanoma skin cancers, non-Hodgkin lymphoma, acute myeloid leukaemia and urinary tract cancers have been reported, it is generally believed that these are related to certain immunosuppressing therapies that have historically been used to treat the disease (5,7,8). For example, the use of thiopurines for IBD is associated with a 1.3–1.7 overall relative risk of cancer and this is reversible upon the discontinuation of therapy (9,10).

Given the clear effects IBD has on gastrointestinal tissues, and the less-compelling inflammation and other carcinogenesis-related effects in distal tissues, it was noteworthy that Westbrook *et al.* (11) observed what they termed evidence of systemic genotoxicity in mouse models of IBD. These investigators reported elevated frequencies of micronucleated (MN) normochromatic erythrocytes in chemical- and immune-mediated colitis mouse models, and they also observed 8-oxoguanine- and γH2AX-positive leukocytes.

We sought to extend this work on systemic genotoxicity using the same chemical-induced model of IBD, dextran sulfate sodium salt (DSS) exposure via drinking water. For these studies, mice were treated with up to 4% DSS. Rather than restricting our analyses to normochromatic erythrocytes, we followed Organisation for Economic Cooperation and Development (OECD) Test Guideline 474 which recommends enumerating MN reticulocytes as well (12). We supplemented these assessments of chromosomal damage with the peripheral blood *Pig-a* assay to investigate the potential of an IBD-like condition to induce gene mutation in haematopoietic cells (13). The results of two independent *in vivo* studies are described herein, along with a discussion about the need for additional work in this area.

Materials and methods

Reagents and miscellaneous supplies

DSS (M_r ~ 40 000) was purchased from Sigma-Aldrich, St. Louis, MO. Distilled water was from Erie County Municipal Water Supply, Buffalo, NY (NYSHD Certification No. 197; distributed by Tops Markets, LLC). Reagents used for flow cytometric MN erythrocyte scoring (Anticoagulant Solution, Buffer Solution, DNA Stain, Anti-CD71-FITC and Anti-CD61-PE Antibodies, RNase Solution and Malaria Biostandards) were from *In Vivo* MicroFlow® PLUS M Kits, Litron Laboratories, Rochester, NY. Reagents used for flow cytometric scoring of *Pig-a* mutant phenotype erythrocytes were from Mouse MutaFlow® Kits, Litron Laboratories and included Anticoagulant Solution, Buffer Solution, Nucleic Acid Dye Solution (contains SYTO® 13), Anti-CD24-PE and Anti-CD61-PE. Additional supplies included anti-CD45-PE from BioLegend, San Diego, CA (clone 30-F11), Lympholyte®-Mammal cell separation reagent from Cedarlane, Burlington, NC; Anti-PE MicroBeads, LS Columns and a QuadroMACS™ Separator from Miltenyi Biotec, Bergisch Gladbach, Germany; and CountBright™ Absolute Count Beads from Invitrogen, Carlsbad, CA.

Mice

Experiments were conducted with the oversight of the University of Rochester's Committee for Animal Resources. Male Crl:CD1(ICR) mice were purchased from Charles River Laboratories, Wilmington, MA. Mice were allowed to acclimate for approximately 1 week. Water and food were available *ad libitum* throughout the acclimation and experimental periods.

Treatment and blood harvests: Study 1

Age at the start of treatment was 8 weeks. At this time, groups of eight mice were exposed to DSS via drinking water with 0, 1, 2, 3 or 4% DSS w/v. DSS-containing water bottles were changed every 2–3 days. The treatment period was divided into four intervals whereby mice were alternately treated with DSS-containing solutions for 1 week and then switched to regular drinking water to recover for a one-week period.

Low volume blood samples for the peripheral blood micronucleus assay were collected the same morning when new treatment cycles were initiated: Days 8, 15 and 22. These samples were collected directly into microcentrifuge tubes containing 175 µl MicroFlow PLUS-M kit-supplied Anticoagulant Solution by nicking a lateral tail vein with a surgical blade after animals were warmed briefly under a heat lamp. Samples were maintained at room temperature for less than 3 h until fixation with ultracold methanol as described by Torous *et al.* (14).

Cardiac blood samples were collected on Day 29 for micronucleus and *Pig-a* assays. This was accomplished by exposing one mouse at a time to CO_2 overdose, whereupon the chest cavity was opened and a heparin-coated needle and syringe was used to obtain approximately 1–2 ml blood. Samples were maintained at room temperature for less than 3 h until ultracold methanol fixation occurred to prepare cells for the micronucleus assay. The remaining blood was maintained at 4°C until the samples were processed for the *Pig-a* assay the following day.

Treatment and blood harvests: Study 2

Age at the start of treatment was 8 weeks. At this time, groups of 10 mice were exposed to DSS via drinking water with 0 or 4% DSS w/v. DSS-containing water bottles were changed every 2–3 days. Exposure was maintained and the collection of blood samples for the micronucleus assay was delayed on a mouse-specific basis until rectal bleeding or morbidity was evident (Day 9–18).

Low volume blood samples for the peripheral blood micronucleus assay were collected between Days 9 and 18. These samples were collected as described above. Cardiac blood samples were collected on Day 29 and stored for 1 day as described above for the *Pig-a* assay.

Micronucleus assay: sample preparation and data acquisition

The micronucleus assay provided three key measurements: frequency of CD71-positive reticulocytes, abbreviated RET^{CD71+}; frequency of CD71-positive MN reticulocytes (MN^{CD71+}); and frequency of CD71-negative MN erythrocytes (MN^{CD71-}). These endpoints were scored via flow cytometry according to the *In Vivo* MicroFlow PLUS-M Kit manual, v170503 (www.litronlabs.com). These procedures have been described in detail by Dertinger *et al.* (15). Data were acquired until a user-defined stop-mode was reached: 20 000 RET^{CD71+} per blood sample. Instrument set-up and calibration were performed using kit-supplied biological standards (*Plasmodium berghei*-infected blood cells) (16). A BD FACSCalibur™ flow cytometer running CellQuest™ Pro v5.2 software was used for data acquisition and analysis.

Pig-a assay: sample preparation and data acquisition

The *Pig-a* assay provided three key measurements: frequency of RNA-positive reticulocytes, abbreviated RET^{RNA+}; frequency of CD24-negative reticulocytes (mutant RET); and frequency of CD24-negative erythrocytes (mutant RBC). These endpoints were scored with *In Vivo* Mouse MutaFlow Kit reagents (Litron Laboratories) via immunomagnetic depletion of wild-type erythrocytes and flow cytometric analysis, as described previously (17) and in the *In Vivo* Mouse MutaFlow Kit Instruction Manual, v190109 (www.litronlabs.com).

Pig-a sample labelling and washing steps utilised deep-well 96-well plates from Axygen Scientific (cat. no. P-DW-20-C) which facilitated efficient, parallel processing. Flow cytometric analyses were also conducted using 96-well plates (U-bottom, Corning, cat. no. 3799) and the BD High Throughput Sampler (HTS) provided automated, walk-away flow cytometric analysis.

An Instrument Calibration Standard was created with approximately 50% wild-type and 50% mutant-mimic erythrocytes, and as described previously, it provided a means to rationally and consistently define the location of mutant phenotype cells (18). A BD FACSCanto™ II flow cytometer running BD FACSDiva™ v6.1.2 software was used for data acquisition and analysis.

Data analysis

Change in body weight is expressed in grams; the incidence of RET^{CD71+}, MN^{CD71+}, MN^{CD71-} and RET^{RNA+} are expressed as frequency percent; and mutant RET and mutant RBC values are reported as number per 1 million total RET and RBC, respectively. The formulas used to calculate mutant RET and mutant RBC frequencies were based on pre- and post-immunomagnetic column data as described previously (19) and the MutaFlow manual (www.litronlabs.com).

The effect of treatment on weight and each of the micronucleus and *Pig-a* assay endpoints was evaluated using JMP software (v12.0.1, SAS Institute Inc., Cary, NC). First, each factor was tested for homogeneity of variance using Levene's test (alpha was 0.05). Parametric tests were used when data were found to exhibit homogeneous variances, or when $\log_{10}$ transformation satisfied this criterion. Otherwise, non-parametric tests were applied to untransformed data.

When parametric testing was indicated for Study 1 data, one-way ANOVA was used; when parametric testing was indicated for Study 2 data, a *t*-test was employed. These tests were conducted at alpha 0.05 and in the case of a change in body weight, RET^{CD71+} and RET^{RNA+} they were performed as two-tailed tests. For the MN^{CD71+}, MN^{CD71-}, mutant RET and mutant RBC endpoints, the tests were one-tailed. When ANOVA indicated statistical significance, Dunnett's test was used to identify the responsible group(s) (alpha = 0.05).

When non-parametric testing was indicated for certain Study 1 and Study 2 factors, Kruskal–Wallis and the Wilcoxon test were used, respectively. These tests were conducted at alpha 0.05 and two-tailed in the case of body weight and %RET values, and one-tailed for each of the four genotoxicity endpoints. When Kruskal–Wallis indicated statistical significance, JMP software's Comparisons with Control Using Steel method was used to identify the responsible group(s) (alpha = 0.05).

Results

Study 1

Mean body weight gains over the entire exposure period (Day 1–22) were 3.5, 3.8, 2.7, 3.0 and 1.2 g for the 0, 1, 2, 3 and 4% DSS groups, respectively. Only the reduced weight gains in the 4% DSS group reached statistical significance. Whereas diarrhoea and anal redness were evident in the 3 and 4% DSS groups, only the high-dose group showed obvious signs of rectal bleeding. Bleeding became evident at the end of the first cycle of 4% DSS, resolved when treatment was discontinued and reappeared at the end of the second cycle of DSS.

Micronucleus assay results at four time points are presented in Figure 1. The left-most graphs depict $\%RET^{CD71+}$, with the first three time points showing evidence of a dose-dependent increase. Note that while the Day 22 ANOVA result showed a significant effect, the *post hoc* test was unable to identify the responsible treatment group, likely due to the considerable amount of variation observed in the high-dose animals. Interestingly, the same one high-dose mouse consistently exhibited the highest $\%RET^{CD71+}$ values.

DSS treatment did not have a statistically significant effect on $\%MN^{CD71+}$ (Figure 1, middle graphs) or $\%MN^{CD71-}$ (Figure 1, right-most graphs). While statistical significance was not achieved, it is interesting to note that the same one high-dose mouse that exhibited the highest $\%RET^{CD71+}$ values also exhibited the highest MN^{CD71+} and MN^{CD71-} frequencies on Days 8 and 22, i.e. at the end of the two DSS exposure cycles.

Pig-a mutation assay results for Day 29 blood samples are presented in Figure 2. This was subsequent to a week of recovery, and no difference among treatments groups was found for $\%RET^{RNA+}$ (left-most graphs). DSS treatments also had no discernible effect on the frequency of mutant RET (middle graphs) or mutant RBC (right-most graphs).

Study 2

Change in mean body weights over the exposure periods were 1.9 and –2.6 for the 0 and 4% DSS groups, respectively ($P = 0.0017$). Each of the DSS-exposed mice exhibited diarrhoea and rectal bleeding, but the onset was variable. For instance, whereas half the mice exhibited these severe effects between Days 9 and 12, the other half showed weaker responses that became apparent on Day 18.

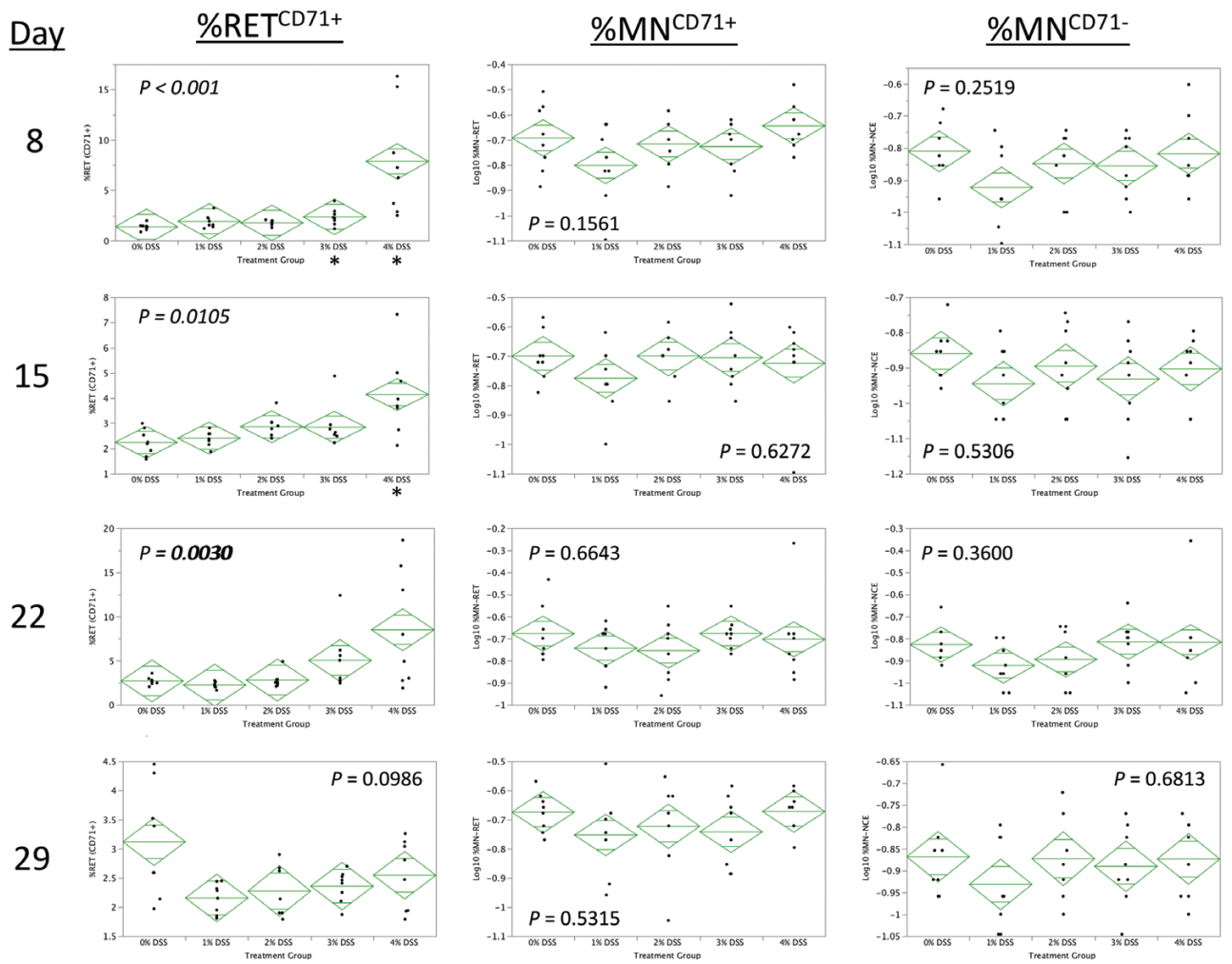

Figure 1. Study 1 micronucleus assay results. The frequency of peripheral blood CD71-positive reticulocytes (RET^{CD71+}), CD71-positive MN reticulocytes (MN^{CD71+}) and CD71-negative MN erythrocytes (MN^{CD71-}) are graphed for each of five DSS treatment groups at each of four time points. Individual points represent individual mice; group mean values are represented by the centre line of each diamond; and the extreme points on each diamond represent upper and lower 95% confidence intervals. The *P*-values provided on each graph correspond to Kruskal–Wallis or ANOVA test results. When treatment was found to be statistically significant ($P < 0.05$), *post hoc* pair-wise testing was conducted and those group(s) found to be significantly different from the 0% DSS control group are indicated by an asterisk.

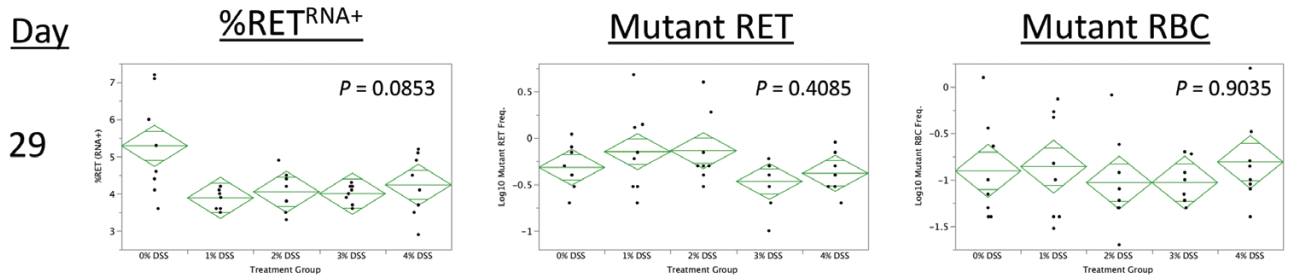

Figure 2. Study 1 *Pig-a* assay results. The frequency of peripheral blood RNA-positive reticulocytes (RET^{RNA+}), mutant reticulocytes (mutant RET) and mutant erythrocytes (mutant RBC) are graphed for each of five DSS treatment groups at one time point. Individual points represent individual mice; group mean values are represented by the centre line of each diamond; and the extreme points on each diamond represent upper and lower 95% confidence intervals. The *P*-values provided on each graph correspond to Kruskal–Wallis or ANOVA test results.

Micronucleus assay results are shown in Figure 3 (top row of graphs). Similar to Study 1, the DSS-treated mice exhibited elevated RET^{CD71+} frequencies at the first blood sampling time. Pair-wise testing showed no evidence for a treatment-related effect on $\%MN^{CD71+}$ or $\%MN^{CD71-}$. Even so, it is perhaps noteworthy that 2 of 10 DSS-treated mice exhibited moderately elevated MN^{CD71+} frequencies: 0.34 and 0.37% (mean ± SEM for the 0% DSS group = 0.20 ± 0.01%). These elevated values were

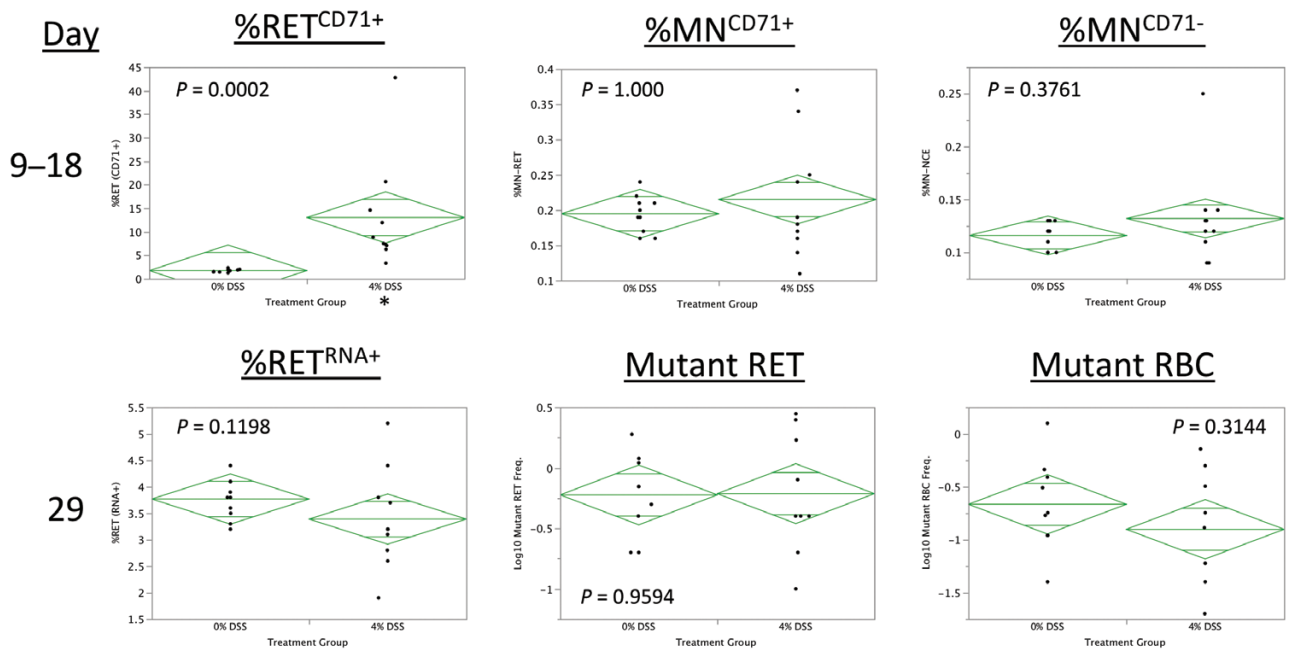

Figure 3. Study 2 micronucleus and *Pig-a* assay results. In the top row, the frequency of peripheral blood CD71-positive reticulocytes (RET^{CD71+}), CD71-positive MN reticulocytes (MN^{CD71+}) and CD71-negative MN erythrocytes (MN^{CD71-}) are graphed for each of two DSS treatment groups at the first blood collection time point. In the bottom row, the frequency of peripheral blood RNA-positive reticulocytes (RET^{RNA+}), mutant reticulocytes (mutant RET) and mutant erythrocytes (mutant RBC) are graphed for each of two DSS treatment groups at Day 29. Individual points represent individual mice; group mean values are represented by the centre line of each diamond; and the extreme points on each diamond represent upper and lower 95% confidence intervals. The *P*-values provided on each graph correspond to Wilcoxon or *t*-test results. Statistically significant differences are indicated by an asterisk.

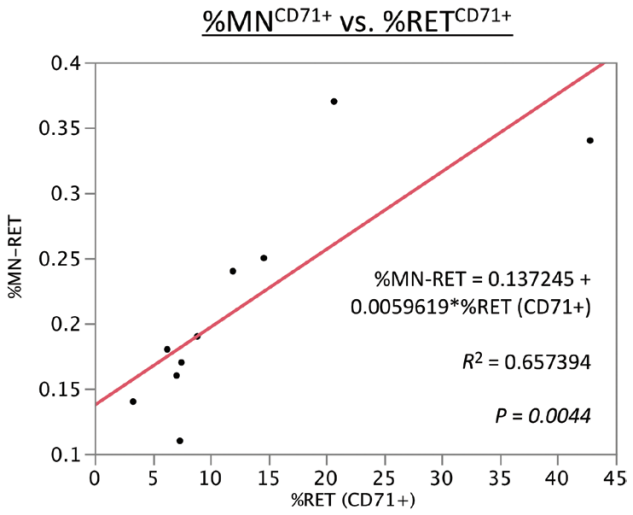

Figure 4. Study 2 micronucleus assay results are shown, with each mouse's CD71-positive MN reticulocyte (MN^{CD71+}) frequency graphed against its corresponding CD71-positive reticulocyte (RET^{CD71+}) frequency. These results are for each 4% DSS-exposed mouse, and the linear fit shows a direct correlation between these factors. The low *P*-value demonstrates that the best-fit line explains the relationship significantly better than a mean fit line.

observed in mice with the highest %RET frequencies. In fact, a best-fit line formed by graphing the 4% DSS group's $\%MN^{CD71+}$ and $\%RET^{CD71+}$ values shows a statistically significant positive correlation ($P = 0.0044$; Figure 4).

Pig-a assay results are shown in Figure 3, the bottom row of graphs. At this late (Day 29) time point, no treatment-related changes to RET^{RNA+}, mutant RET or mutant RBC frequencies were observed.

Discussion

We studied a DSS mouse model of IBD and found evidence of severe gastrointestinal effects, namely diarrhoea and rectal bleeding. We also observed high %RET frequencies in DSS-exposed mice. This was also reported by Trivedi and Jena (20), and as with those investigators, we attribute this to DSS-stimulated erythropoiesis. On the other hand, we were not able to detect DSS treatment-related effects on mutant RET and mutant RBC frequencies. It is noteworthy that there are at least two reports indicating stress erythropoiesis does not affect rodent *Pig-a* mutant cell frequencies (21,22).

We did not observe statistically significant effects of DSS on $\%MN^{CD71+}$ or $\%MN^{CD71-}$. This is inconsistent with reports by Westbrook *et al.* (11) and Trivedi and Jena (20) who found elevated frequencies of MN erythrocytes in mice exposed to DSS in drinking water. There are several non-mutually exclusive explanations for the divergent results. Mouse strains used for these various studies were different, and it has been reported that factors including the gut microbiome and cleanliness of the vivarium can impact the responsiveness of mice to DSS (23). It is also possible that the variability of the DSS animals' responsiveness adversely affected our ability to detect significant genotoxic effects. That being said, in each instance MN^{CD71+} values were moderately elevated, it was always in conjunction with remarkably high $\%RET^{CD71+}$ values. One interpretation of these results is that stimulated erythropoiesis is responsible for elevated frequencies of MN erythrocyte populations. Indeed, as reviewed by Tweats *et al.* (24), it is well known that high erythropoiesis function itself is capable of increasing MN erythrocyte

frequencies. To the extent one embraces this view, DSS-induced IBD cannot be considered a systemic genotoxicant, but rather an indirect inducer of micronuclei as a consequence of stress erythropoiesis.

Effects of oral DSS treatment on peripheral blood leukocytes have been reported that lend some support to the systemic genotoxicity hypothesis. For instance, Westbrook *et al.* (11) demonstrated that leukocytes from DSS-treated mice showed increased labelling for γH2AX and 8-oxoguanine. Even so, attributing these results to systemic genotoxicity is also problematic. Through elaborate processes that involve adhesion molecules and chemokine receptors, IBD causes the recruitment of leukocytes from the bloodstream to the intestine (25–27). Once in the gastrointestinal tract, transmigration through blood vessels occurs, thereby allowing immune cells to come into contact with antigen-presenting cells. This homing process does not permanently anchor leukocytes to gastrointestinal tissue. Rather, they are observed to migrate to regional lymph nodes and to the systemic circulation via the thoracic duct (27). Therefore, assaying blood leukocytes does not completely solve the challenge of differentiating genotoxicity that is occurring locally in inflamed tissue(s) versus DNA damage that is occurring systemically.

Additional work is needed to more thoroughly investigate systemic effects associated with IBD-like conditions, including genotoxicity. Given the confounding influence that stimulated erythropoiesis has on MN erythrocyte assays, future rodent-based studies would benefit from the evaluation of distal tissues in addition to gastrointestinal and haematopoietic cells (28–30). Furthermore, beyond relying on rodent models, it would be most ideal to extend these studies to include analyses of CD and UC patients before and during the course of therapy. This is possible for several genotoxicity endpoints that can be applied across mammalian species of toxicological interest (29,31–33). For instance, at the time of this writing, Cao *et al.* (34) reported that Chinese IBD patients experiencing azathioprine-based therapy showed slightly elevated frequencies of *Pig-a* mutant cells and pronounced increases in MN lymphocytes. However, since all of the IBD patients were actively being treated with azathioprine, it is not possible to ascribe these findings to the disease as opposed to the known *in vivo* genotoxicity of the drug (19). This reinforces the need for additional studies that are designed to discriminate genotoxic effects associated with IBD itself versus those caused by the therapeutic intervention(s).

Funding

This work was funded by grants from the National Institutes of Health/National Institute of Environmental Health Sciences (NIEHS; grant no. R44ES028163). The contents are solely the responsibility of the authors and do not necessarily represent the official views of the NIEHS.

Conflict of interest statement: C.K., S.L.A., D.K.T., S.T., P.S., J.C.B. and S.D.D. are employees of Litron Laboratories. Litron holds patents covering flow cytometric methods for scoring micronucleated erythrocytes and sells kits based on this technology (*In Vivo* MicroFlow®); Litron holds patents for scoring GPI anchor-deficient erythrocytes and sells kits based on this technology (*In Vivo* MutaFlow®).

References

1. Abraham, C. and Cho, J. H. (2009) Inflammatory bowel disease. *N. Engl. J. Med.*, 361, 2066–2078.
2. Jess, T., Rungoe, C. and Peyrin-Biroulet, L. (2012) Risk of colorectal cancer in patients with ulcerative colitis: a meta-analysis of population-based cohort studies. *Clin. Gastroenterol. Hepatol.*, 10, 639–645.
3. Eaden, J. A., Abrams, K. R. and Mayberry, J. F. (2001) The risk of colorectal cancer in ulcerative colitis: a meta-analysis. *Gut*, 48, 526–535.
4. Annese, V., Beaugerie, L., Egan, L., *et al.*; ECCO. (2015) European evidence-based consensus: inflammatory bowel disease and malignancies. *J. Crohns. Colitis.*, 9, 945–965.
5. Axelrad, J. E., Lichtiger, S. and Yajnik, V. (2016) Inflammatory bowel disease and cancer: the role of inflammation, immunosuppression, and cancer treatment. *World J. Gastroenterol.*, 22, 4794–4801.
6. Hanahan, D. and Weinberg, R. A. (2011) Hallmarks of cancer: the next generation. *Cell*, 144, 646–674.
7. Jones, J. L. and Loftus, E. V. Jr. (2007) Lymphoma risk in inflammatory bowel disease: is it the disease or its treatment? *Inflamm. Bowel Dis.*, 13, 1299–1307.
8. Pedersen, N., Duricova, D., Elkjaer, M., Gamborg, M., Munkholm, P. and Jess, T. (2010) Risk of extra-intestinal cancer in inflammatory bowel disease: meta-analysis of population-based cohort studies. *Am. J. Gastroenterol.*, 105, 1480–1487.
9. Pasternak, B., Svanström, H., Schmiegelow, K., Jess, T. and Hviid, A. (2013) Use of azathioprine and the risk of cancer in inflammatory bowel disease. *Am. J. Epidemiol.*, 177, 1296–1305.
10. Beaugerie, L., Carrat, F., Colombel, J. F., *et al.*; CESAME Study Group. (2014) Risk of new or recurrent cancer under immunosuppressive therapy in patients with IBD and previous cancer. *Gut*, 63, 1416–1423.
11. Westbrook, A. M., Wei, B., Braun, J. and Schiestl, R. H. (2009) Intestinal mucosal inflammation leads to systemic genotoxicity in mice. *Cancer Res.*, 69, 4827–4834.
12. OECD (Organisation for Economic Cooperation and Development). (2016) *OECD Guideline for the Testing of Chemicals: Mammalian Erythrocyte Micronucleus Test. Test Guideline 474*. https://www.oecd-ilibrary.org/docserver/9789264264762-en.pdf?expires=1573489961&id=id&accname=guest&checksum=03E6EB119F8BE1D262013FF07E78236F. (accessed November 11, 2019).
13. Gollapudi, B. B., Lynch, A. M., Heflich, R. H., *et al.* (2015) The in vivo *Pig-a* assay: a report of the International Workshop On Genotoxicity Testing (IWGT) workgroup. *Mutat. Res. Genet. Toxicol. Environ. Mutagen.*, 783, 23–35.
14. Torous, D. K., Hall, N. E., Murante, F. G., Gleason, S. E., Tometsko, C. R. and Dertinger, S. D. (2003) Comparative scoring of micronucleated reticulocytes in rat peripheral blood by flow cytometry and microscopy. *Toxicol. Sci.*, 74, 309–314.
15. Dertinger, S. D., Camphausen, K., Macgregor, J. T., *et al.* (2004) Three-color labeling method for flow cytometric measurement of cytogenetic damage in rodent and human blood. *Environ. Mol. Mutagen.*, 44, 427–435.
16. Tometsko, A. M., Torous, D. K. and Dertinger, S. D. (1993) Analysis of micronucleated cells by flow cytometry. 1. Achieving high resolution with a malaria model. *Mutat. Res.*, 292, 129–135.
17. Maurice, C., Dertinger, S. D., Yauk, C. L. and Marchetti, F. (2019) Integrated in vivo genotoxicity assessment of procarbazine hydrochloride demonstrates induction of *Pig*-a and *LacZ* mutations, and micronuclei, in MutaMouse hematopoietic cells. *Environ. Mol. Mutagen.*, 60, 505–512.
18. Phonethepswath, S., Franklin, D., Torous, D. K., *et al.* (2010) *Pig-a* mutation: kinetics in rat erythrocytes following exposure to five prototypical mutagens. *Toxicol. Sci.*, 114, 59–70.
19. Dertinger, S. D., Phonethepswath, S., Avlasevich, S. L., *et al.* (2012) Efficient monitoring of in *vivo Pig-a* gene mutation and chromosomal damage: summary of 7 published studies and results from 11 new reference compounds. *Toxicol. Sci.*, 130, 328–348.
20. Trivedi, P. P. and Jena, G. B. (2012) Dextran sulfate sodium-induced ulcerative colitis leads to increased hematopoiesis and induces both local as well as systemic genotoxicity in mice. *Mutat. Res.*, 744, 172–183.
21. Kenyon, M. O., Coffing, S. L., Ackerman, J. I., Gunther, W. C., Dertinger, S. D., Criswell, K. and Dobo, K. L. (2015) Compensatory erythropoiesis has no impact on the outcome of the in vivo *Pig-a* mutation assay in rats following treatment with the haemolytic agent 2-butoxyethanol. *Mutagenesis*, 30, 325–334.

22. Nicolette, J., Murray, J., Sonders, P. and Leroy, B. (2018) A regenerative erythropoietic response does not increase the frequency of *Pig-a* mutant reticulocytes and erythrocytes in Sprague-Dawley rats. *Environ. Mol. Mutagen.*, 59, 91–95.
23. Perše, M. and Cerar, A. (2012) Dextran sodium sulphate colitis mouse model: traps and tricks. *J. Biomed. Biotechnol.*, 2012, 718617.
24. Tweats, D. J., Blakey, D., Heflich, R. H., *et al.*; IWGT Working Group. (2007) Report of the IWGT working group on strategies and interpretation of regulatory in vivo tests I. Increases in micronucleated bone marrow cells in rodents that do not indicate genotoxic hazards. *Mutat. Res.*, 627, 78–91.
25. Butcher, E. C. and Picker, L. J. (1996) Lymphocyte homing and homeostasis. *Science*, 272, 60–66.
26. Eksteen, B., Liaskou, E. and Adams, D. H. (2008) Lymphocyte homing and its role in the pathogenesis of IBD. *Inflamm. Bowel Dis.*, 14, 1298–1312.
27. Fischer, A., Zundler, S., Atreya, R., *et al.* (2016) Differential effects of α4β7 and GPR15 on homing of effector and regulatory T cells from patients with UC to the inflamed gut in vivo. *Gut*, 65, 1642–1664.
28. Lambert, I. B., Singer, T. M., Boucher, S. E. and Douglas, G. R. (2005) Detailed review of transgenic rodent mutation assays. *Mutat. Res.*, 590, 1–280.
29. Tice, R. R., Agurell, E., Anderson, D., *et al.* (2000) Single cell gel/comet assay: guidelines for in vitro and in vivo genetic toxicology testing. *Environ. Mol. Mutagen.*, 35, 206–221.
30. Uno, Y., Morita, T., Luijten, M., Beevers, C., Hamada, S., Itoh, S., Ohyama, W. and Takasawa, H. (2015) Recommended protocols for the liver micronucleus test: report of the IWGT working group. *Mutat. Res. Genet. Toxicol. Environ. Mutagen.*, 783, 13–18.
31. Salk, J. J. and Kennedy, S. R. (2020) Next-generation genotoxicity: using modern sequencing technologies to assess somatic mutagenesis and cancer risk. *Environ. Mol. Mutagen.*, 61, 135–151.
32. Dertinger, S. D., Miller, R. K., Brewer, K., *et al.* (2007) Automated human blood micronucleated reticulocyte measurements for rapid assessment of chromosomal damage. *Mutat. Res.*, 626, 111–119.
33. Dertinger, S. D., Avlasevich, S. L., Bemis, J. C., Chen, Y. and MacGregor, J. T. (2015) Human erythrocyte *Pig-a* assay: an easily monitored index of gene mutation requiring low volume blood samples. *Environ. Mol. Mutagen.*, 56, 366–377.
34. Cao, Y., Wang, X., Liu, W., *et al.* (2020) The potential application of human *PIG-A* assay on azathioprine-treated inflammatory bowel disease patients. *Environ. Mol. Mutagen.*, in press, doi:10.1002.em.22348.